PHYSICAL REVIEW B VOLUME 18, NUMBER 3 1 AUGUST 1978

Experimental study of flux peaking for channeled ions using ^{18}O in Ti

R. B. Alexander*
Institute of Physics, University of Aarhus, DK 8000 Aarhus C, Denmark

R. J. Petty†
Nuclear Physics Division, A.E.R.E., Harwell, United Kingdom
(Received 9 May 1977)

An experimental study has been made of the flux-peaking effect for channeled ions in ^{18}O-implanted Ti single crystals. Using 730-keV protons, as well as H_2^+ and H_3^+ ions of the same velocity, the angular dependence of the ^{18}O $(p,\alpha)^{15}N$ reaction yield has been measured in scans across the [0001] and $\langle 11\bar{2}0\rangle$ axes and the (0001) plane. It is found that the implanted O occupies the same octahedral interstitial sites in Ti as in diffused samples. The dependence of the flux peak in the ^{18}O yield on various factors has been investigated. While the magnitude of the peak is extremely sensitive to any factors which increase the transverse energy of the best-channeled ions, the width is relatively insensitive. For both the [0001] and $\langle 11\bar{2}0\rangle$ axes, the transition from axial to planar flux peaking has been examined. The magnitude of the flux peak for the (0001) plane is found to be greater than that for the $\langle 11\bar{2}0\rangle$ axis intersected by the plane. This is opposite to the behavior predicted by theoretical calculations, using both an analytical model and computer simulation, for channeling in Cu. Possible explanations for the discrepancy are discussed.

I. INTRODUCTION

The existence of flux peaking for ions channeled in a single crystal[1] is now well established. An understanding of the flux-peaking effect is important in applications of channeling and blocking, such as the lattice location of foreign atoms[2] and the measurement of compound nuclear lifetimes,[3] as well as in more basic channeling studies. Although several theoretical studies of the effect have been made, little experimental work has yet been carried out. Channeling flux distributions are most easily probed experimentally by measuring the yield of some close-impact process from interstitial foreign atoms. The energy and depth dependence of flux peaking have been investigated in this way using Yb implanted in Si,[4] but the Yb atoms do not occupy a unique flux-peaking site. In another investigation, the influence of interstitial O atoms on the channeling flux distribution in Ti was examined,[5,6] but only at high O concentrations ($\geq$10 at.%).

Our aim in the present work was to study flux peaking experimentally in a known dilute interstitial system. A suitable system is the solid solution of O in Ti (as used in Refs. 5 and 6), in which the O atoms are known to occupy the octahedral interstitial sites in the hcp α-Ti lattice.[7] Because of difficulties previously experienced in diffusing O into Ti,[8] Ti crystals were implanted with ^{18}O (dose 5×10^{14} ions cm^{-2}). It is found that the implanted O occupies the same interstitial sites as in diffused samples.

Channeling measurements have been made with 730-keV protons, as well as H_2^+ and H_3^+ ions of the same velocity, the ^{18}O being detected by the $^{18}O(p,\alpha)^{15}N$ reaction. Angular scans have been carried out across the [0001] and $\langle 11\bar{2}0\rangle$ axes and the (0001) plane in Ti. Strong flux-peaking effects are observed in each case. For the [0001] axis, the dependence of the flux peak on factors affecting the transverse energy of the channeled ions has been investigated. For both the [0001] and $\langle 11\bar{2}0\rangle$ axes, the transition from axial to planar flux peaking has been studied. In the case of the $\langle 11\bar{2}0\rangle$-(0001) transition, the flux peak is higher for the plane than the axis.

To investigate this effect, theoretical calculations of the flux peaking in a $\langle 110\rangle$-$\{111\}$ transition in Cu have been performed, using both an analytical model and computer simulation. Cu was chosen because the $\langle 110\rangle$ channels in Cu are almost identical to the $\langle 11\bar{2}0\rangle$ channels in Ti, and because a computer program was already available. Various possible explanations of the high planar flux peaking observed in Ti are discussed.

II. EXPERIMENTAL PROCEDURE

A. Crystal preparation

The Ti single crystals used in this work (supplied by Metals Research Ltd.) were thin disks, approximately 6 mm in diameter and 1 mm thick, cut with either a [0001] or $\langle 11\bar{2}0\rangle$ axis approximately normal to the surface. The Ti purity was 99.9%. After mechanical (including vibratory) polishing, the crystals were electropolished in a solution of 5% perchloric acid and 95% acetic anhydride. Successful electropolishing proved dif-

ficult. The best results were obtained with the electrolyte temperature between −20 and −15 °C and the cell voltage in the range 30–40 V, corresponding to the current plateau; a Pt cathode was used. Crystals electropolished under these conditions had channeling minimum yields < 0.05.

Implantation of ^{18}O was carried out on the Harwell Mk.I separator at 35 keV. The energy was chosen so that the ^{18}O range would correspond to the first maximum in the flux-peaking depth distribution[4,9] for 730-keV protons channeled along the [0001] axis, thereby maximizing the flux-peaking effect for this direction. The depth of the maximum, calculated using the static continuum form of the Molière potential function[10] to determine the [0001] transverse potential, is 510 Å. At an implantation energy of 35 keV, the calculated projected range $\bar{R}_p$ of the ^{18}O ions is 525 Å with a standard deviation $\Delta\bar{R}_p$ of 260 Å.[11] Implants were performed at room temperature with the ions incident at 7° to the surface normal. The dose was 5×10^{14} ions cm^{-2}, giving an average concentration of 0.14 at.% ^{18}O in the implanted region.

Radiation damage resulting from implantation affects flux peaking (cf. Sec. III A). Consequently, annealing of the implanted crystals to reduce the damage would have been desirable. However, even at a temperature of 400 °C, the diffusion coefficient for O in α-Ti is sufficiently high[12] that a substantial fraction of the implanted O would diffuse to the crystal surface in a 15-min anneal. It was found that annealing one crystal at 350 °C for 30 min had only a very small effect on both the damage (as indicated by the Ti minimum yield) and the flux peaking.

B. Experimental arrangement

Two accelerators were used for the experiments: the 2-MV Van de Graaff at the University of Aarhus, to produce 730-keV H^+ ions, and the 5-MV Van de Graaff at AERE, Harwell, to produce 1.46-MeV H_2^+ and 2.19-MeV H_3^+ ions. Deuterium contamination of the H_2^+ and H_3^+ beams was determined (using scattering from a thin Au foil) to be <0.3%. For proton energies near 730 keV, the cross section of the $^{18}O(p, \alpha)^{15}N$ reaction is approximately constant with energy.[13,14] The differential cross section at backward angles is ~14 mb/sr and the reaction Q value is 3.97 MeV.

Similar experimental arrangements were employed in both cases. The incident beam was collimated to a size of 0.8 mm and an angular divergence half-width of <0.03°. Crystal alignment and angular scans were carried out using a three-axis goniometer, controlled by stepping motors which allowed target rotations as small as 0.01°. A secondary electron suppressor in the form of a wire loop was mounted close to the target. The target was surrounded by a shield cooled with liquid nitrogen to minimize surface contamination, and the target chamber vacuum was $\lesssim 10^{-6}$ Torr.

Two Si surface-barrier detectors were used. A 300-mm^2 detector, located at a scattering angle of ~145° and subtending a large solid angle ~0.4 sr, detected the emergent α particles. To absorb the very large number of backscattered protons the detector was covered with a 12-μm Mylar foil[14]; this reduced the α-particle energy of 3.4 MeV by ~2.6 MeV. The second detector, 25 mm^2 in area and at a scattering angle of 165°, measured the backscattered proton yield. This was covered with an Al foil in which a number of small holes had been made, so as to keep the count rate low while avoiding blocking effects.

Typical beam currents were 100–200 nA. In order to avoid large ion doses and consequent radiation damage during crystal alignment, a 1.8-MeV-proton beam was used for alignment. Protons of this energy backscattered from the surface region of the Ti could penetrate the Mylar foil covering the large solid angle detector. Thus alignment could be performed at low beam currents (~0.2 nA) by monitoring the proton yield in this detector.

III. RESULTS AND DISCUSSION

An α-particle energy spectrum for 730-keV protons incident in a random direction is shown in Fig. 1. Similar spectra were obtained for H_2^+ and H_3^+ ions, except for a low-energy continuum thought to be due to backscattering from the Ti of contaminant deuterium.

The α-particle counts were summed over the energy window indicated in Fig. 1. Since the depth resolution is limited by energy straggling in the Mylar absorber to ~2000 Å, the contributions to the α-particle yield from the implanted ^{18}O and from natural ^{18}O (isotopic abundance 0.2%) in the surface oxide layer cannot be distinguished. The contribution from surface ^{18}O was estimated, from measurements on an unimplanted crystal, to be 10–15% of the total yield. For the implanted crystals, the oxide contribution could have been determined by means of the $^{16}O(d, p)^{17}O$ reaction. However, as this could not be done simultaneously with the $^{18}O(p, \alpha)^{15}N$ measurements, no correction for surface ^{18}O was made to the observed α-particle yields. The Ti yield was determined in a window set on the backscattered proton spectrum, at an energy corresponding to scattering from Ti at the (calculated) depth of the implanted O.

Typical ion doses at each position in the angular

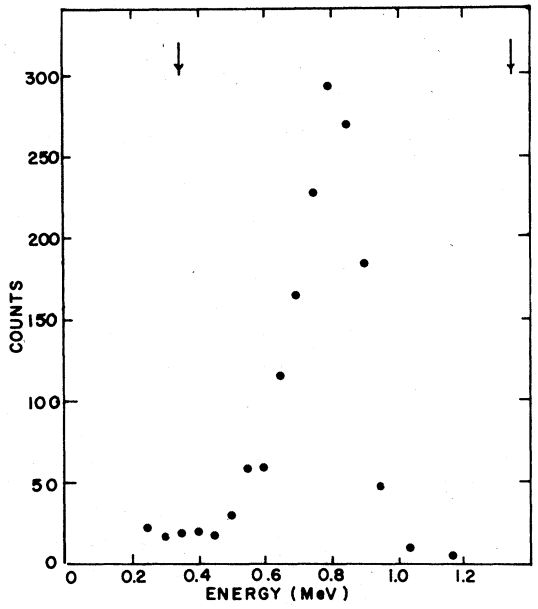

FIG. 1. Energy spectrum of α particles from the $^{18}O(p,\alpha)^{15}N$ reaction, for 730-keV protons incident in a random direction in a Ti single crystal implanted with ^{18}O. The α-particle detector was covered with a 12-μm Mylar foil.

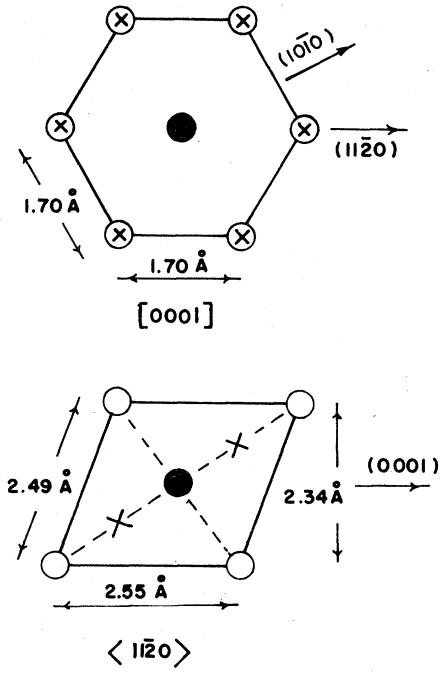

FIG. 2. Cross sections of the [0001] and ⟨11$\bar{2}$0⟩ axial channels in Ti. Open circles represent rows of Ti atoms. The filled circles and crosses denote the projections of the octahedral and tetrahedral interstitial sites, respectively, on planes normal to the channels.

scans were 20–30 μC. The corresponding ^{18}O random yield levels were approximately 400–600 counts.

A. Axial flux peaking

The geometry of the [0001] and ⟨11$\bar{2}$0⟩ axial channels in Ti is illustrated in Fig. 2, which also shows the positions of the octahedral and tetrahedral interstitial sites. Figure 3 shows the results of angular scans carried out across the two axes with 730-keV protons; the tilting planes for the scans are included in Table I. The widths of the Ti dips are in reasonable agreement with the values predicted by the calculations of Barrett.[15]

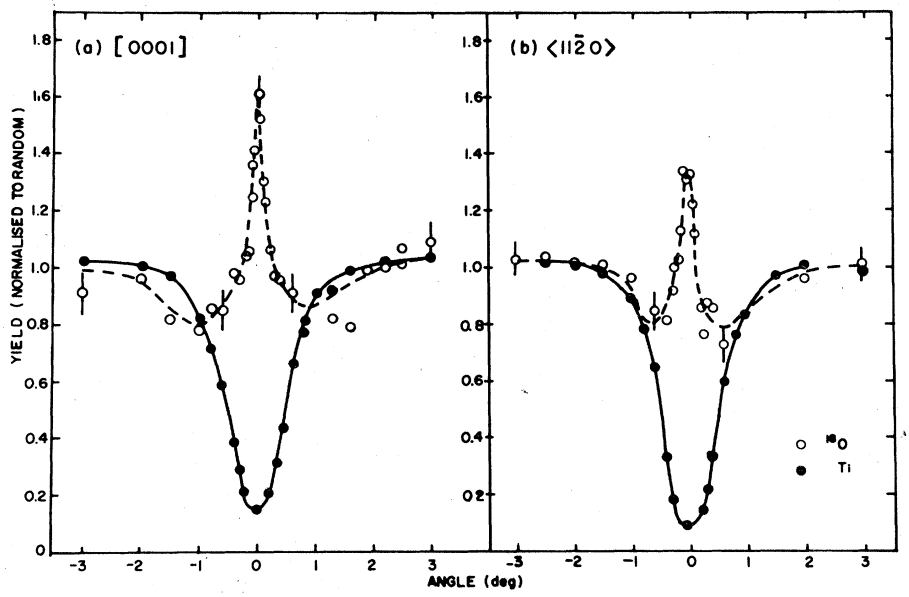

FIG. 3. Angular scans carried out with 730-keV protons across (a) the [0001] axis and (b) a ⟨11$\bar{2}$0⟩ axis in ^{18}O-implanted Ti single crystals. The open circles correspond to the α-particle nuclear-reaction yield from ^{18}O, and the filled circles to the proton backscattering yield from Ti. Some of the data points have been omitted for clarity.

TABLE I. Experimental parameters for the axial and planar angular scans. χ_0 is the normalized aligned yield, and $\psi_{1/2}$ is the half-width at half-maximum (half-minimum) of the O peak (Ti dip). Errors in χ_0(Ti) are <0.005. The value of the maximum flux F_{max} for the axial measurements is defined by Eq. (2).

Channel	Incident ion	χ_0(O)	χ_0(Ti)	$\psi_{1/2}$(O) (deg)	$\psi_{1/2}$(Ti) (deg)	F_{max}	Tilting plane
[0001]	730-keV H^+	1.64 ±0.06	0.13	0.105 ±0.01	0.56 ±0.02	1.74 ±0.07	8.5° from $\{11\bar{2}0\}$
	1.46-MeV H_2^+	1.61 ±0.08	0.21	0.15 ±0.03	0.65 ±0.05	1.77 ±0.10	~10° from $\{11\bar{2}0\}$
	2.19-MeV H_3^+	1.25 ±0.04	0.34	0.17 ±0.05	0.65 ±0.05	1.38 ±0.06	~10° from $\{11\bar{2}0\}$
$\langle 11\bar{2}0\rangle$	730-keV H^+	1.33 ±0.06	0.089	0.11 ±0.03	0.53 ±0.02	1.36 ±0.07	14° from $\{10\bar{1}0\}$
	1.46-MeV H_2^+	1.24 ±0.06	0.20	0.13 ±0.05	0.50 ±0.02	1.30 ±0.08	18° from $\{10\bar{1}0\}$
(0001)	730-keV H^+	1.50 ±0.05	0.31	0.11 ±0.02	0.26 ±0.02		8° from $\langle 11\bar{2}0\rangle$

In both scans a strong central flux peak is seen in the ^{18}O yield, with an angular width ~0.2 of the Ti dip width. That the implanted O occupies octahedral sites in the Ti lattice is confirmed by the narrow flux peaks observed for the two axes, together with the flux peak observed for the (0001) plane (see Sec. III B). The possibility of a tetrahedral component is excluded by the lack of sideband peaks in the $\langle 11\bar{2}0\rangle$ scan. Both the axial flux peaks appear to be superimposed on dips, suggesting that some of the O is substitutional, but the "dips" are much too wide for this to be the case. Rather, the flux peaks are flanked by inverted shoulders or compensating troughs.

The magnitude of the [0001] flux peak is 1.64 ±0.06, comparable to the largest values observed for interstitial impurities in lattice location experiments.[2] Although the ^{18}O range corresponds to the first maximum in the flux-peaking depth distribution for the [0001] axis (Sec. II A), the observed flux peaking will be less than the maximum because of range straggling together with the limited experimental depth resolution. Investigation of the depth dependence of the flux peaking is precluded by the depth resolution. It should be noted that the surface ^{18}O background contribution discussed previously also results in the observed flux peak being slightly smaller than its actual value.

Analytical treatments of flux peaking based on the continuum model have been given by Van Vliet[9] and Kumakhov.[16,17] In axial channeling, the maximum flux F_{max} can be expressed as

$$F_{max} \approx 1 + \ln(A_0 k/\Pi \delta E_\perp), \quad (1)$$

in which A_0 is the channel cross-sectional area, and $\delta E_\perp$ is the fluctuation in transverse energy of the best-channeled ions due to multiple scattering. The constant k is defined by $U(\rho) = k\rho^2$, where $U(\rho)$ is the transverse potential (about the channel symmetry axis) in the harmonic approximation. Using a Molière continuum potential, substitution in Eq. (1) of the value $F_{max} = 1.74$ deduced for the [0001] axis (Table I) gives $\delta E_\perp = 7.9$ eV. In these experiments the major sources of multiple scattering are implantation damage and the surface oxide layer. The half-width (at half-maximum) of the [0001] flux peak is 0.11°, ~30% less than theoretical estimates.[9,16] For the $\langle 11\bar{2}0\rangle$ axis, Eq. (1) cannot be applied as the potential is not symmetric about the channel center.

Angular scans across the [0001] and $\langle 11\bar{2}0\rangle$ axes were also carried out with 1.46-MeV H_2^+ ions, and across the [0001] axis with 2.19-MeV H_3^+ ions. The molecular ions have the same velocity as 730-keV protons. Differences in the flux peaking (and the channeling behavior) might be expected for molecular ions, due to the transverse energy imparted to the protons by the breakup of the molecules as they enter the crystal.

Scans across the [0001] axis with protons and H_3^+ ions are compared in Fig. 4. The H_2^+ scan (not shown) was almost identical to the proton scan, except that the Ti dip was somewhat wider, probably due to the choice of tilting plane. The Ti dip in the H_3^+ scan, carried out in the same plane, shows a similar effect. It is seen that the Ti minimum yield for H_3^+ is considerably higher than for protons. This is consistent with the observations of Tombrello *et al.*[18,19] for H_3^+ channeling in Si, though the high minimum yield may arise partly from poor crystal surface conditions for the scan here.

Table I summarizes the results of all the angular scans [including the (0001) planar scan]. The maximum flux F_{max} in axial channeling is, to a first approximation, the flux-peak magnitude corrected for the random fraction of the incident beam arising from dechanneling:

$$F_{max} = [\chi_0(0) - \chi_0(\mathrm{Ti})]/[1 - \chi_0(\mathrm{Ti})], \quad (2)$$

where χ_0 is the normalized yield in the aligned direction.

The most significant feature of the H_3^+ results is that F_{max} is reduced by a factor of about 2 compared to protons. A similar effect was reported by

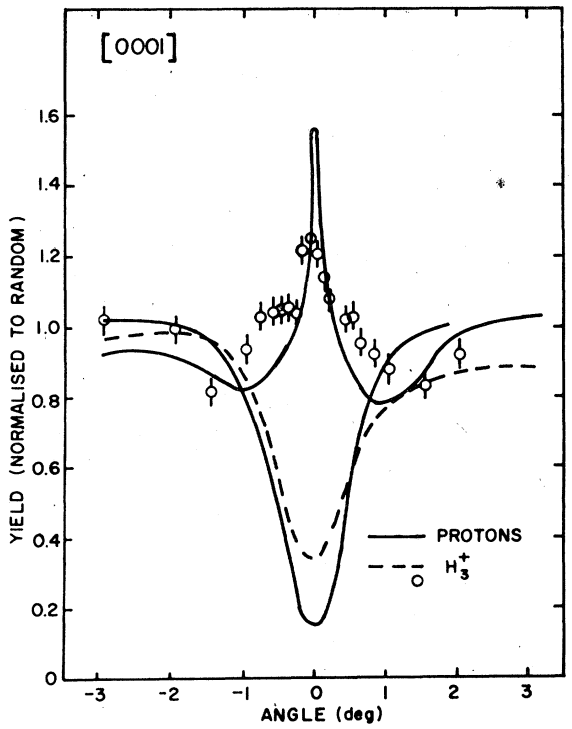

FIG. 4. Comparison of angular scans across the [0001] axis for 730-keV protons and 2.19-MeV H_3^+ ions. For clarity, only the H_3^+ data points for ^{18}O are shown.

Eisen and Uggerhøj[4] in their study of Yb-implanted Si. Using Eq. (1), the transverse energy of the best-channeled ions corresponding to the reduction in flux peaking is ~3 eV. Hence the contribution to the transverse energy per proton from the breakup of a H_3^+ molecule is of this order, while for H_2^+ (for which no reduction in flux peaking is observed) the contribution must be smaller. Assuming a simple Coulomb explosion, the maximum contribution to the transverse energy per proton, calculated from the Coulomb potential energy, is 4.5 eV for H_2^+ and 11.0 eV for H_3^+. However, these maximum values will not be attained at the depth of the implanted O($\overline{R}_p$ = 525 Å), where the interproton separation in the molecular cluster is estimated (using Ref. 20, Fig. 4) to be only about 2–3 times the initial separation. Furthermore, quantitative estimates of the transverse energy are complicated by the influence of the transverse "wake" force believed to act on the trailing particles in a cluster.[21] Another feature of the H_2^+ and H_3^+ results is that the flux peak appears to be slightly wider than for protons. This effect may be associated with the width of the Ti dip.

One of the major factors affecting the transverse energy of the best-channeled ions, and thus the flux peaking, is multiple scattering arising from

TABLE II. Normalized aligned yields χ_0(O) and χ_0(Ti) for the [0001] axis, and values of F_{max} [Eq. (2)], as a function of 730-keV proton dose. Errors in χ_0(Ti) are <0.005. The beam-spot area was 0.8×0.8 mm^2.

Dose (μC)	χ_0(O)	χ_0(Ti)	F_{max}
60	1.64±0.06	0.13	1.74±0.07
1000	1.54±0.06	0.18	1.66±0.07
1350	1.48±0.06	0.19	1.59±0.07
1650	1.34±0.06	0.20	1.43±0.07

radiation damage. To investigate this, the magnitude of the [0001] flux peak was measured as a function of bombardment dose for 730-keV protons. The results are given in Table II. While χ_0(Ti) increases slightly with dose, the value of F_{max}, which takes the dechanneling associated with this increase into account, decreases rapidly. This illustrates the extreme sensitivity of the magnitude of a flux peak to small levels of damage, as found earlier in the work of Andersen *et al.*[22] Additional measurements made at nonzero angles of incidence indicated that the width of the flux peak remained constant as the magnitude decreased, at least within the limits of experimental error. The relative insensitivity of the peak width to multiple scattering, previously found in computer-simulation studies,[8] is predicted by analytical models.[9,16] We note here that with increasing thermal vibrational amplitude of an impurity at the center of a channel, the flux-peak width increases as the magnitude decreases.[23]

Because of the dependence of the peak height on radiation damage, the central points in each angular scan were always measured first. No effects were observed during the scans which suggested any change in the location of the implanted O.

B. Planar flux peaking

Figure 5 shows the results of an angular scan across the (0001) plane using 730-keV protons. Again a strong flux peak is seen in the ^{18}O yield, but the width is considerably larger compared to the Ti dip width than in the axial scans. This reflects the steeper transverse potential gradient about the channel axis for planes compared to axes.

The magnitude of the flux peak is comparable to the values calculated from the theoretical expressions of Morgan and Van Vliet[24] and Kumakhov,[17] assuming that $\delta E_\perp = 7.9$ eV as determined from the axial results. However, an unexpected feature of the results is that the flux-peak magnitude for the (0001) plane is greater than that for the $\langle 11\bar{2}0 \rangle$ axis which is intersected by the plane [cf. Figs. 3(b) and 6(c)].

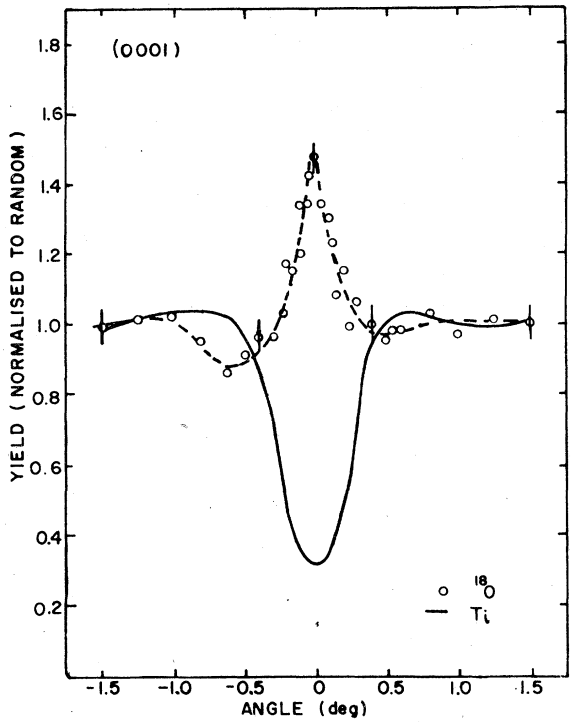

FIG. 5. Angular scan across the (0001) plane, with the same conditions as for Fig. 3.

C. Transition from axial to planar flux peaking

To investigate the transition from axial to planar flux peaking, angular scans were carried out (with 730-keV protons) across the [0001] axis in $\{11\bar{2}0\}$ and $\{10\bar{1}0\}$ planes, and across the $\langle 11\bar{2}0\rangle$ axis in the (0001) plane. The results are presented in Fig. 6.

As shown in Fig. 2 the octahedral interstitial site lies at the center of $\{10\bar{1}0\}$ and (0001) planar channels, but is completely shadowed along $\{11\bar{2}0\}$ channels. Thus planar flux peaking would only be expected in the $\{10\bar{1}0\}$ and (0001) scans. In the [0001]-$\{11\bar{2}0\}$ scan, the ^{18}O yield displays a central axial flux peak and tends towards the host Ti yield at angles $>\psi_{1/2}$(Ti), as expected for atoms shadowed with respect to the planes. In the [0001]-$\{10\bar{1}0\}$ scan, the ^{18}O yield displays both axial and planar flux peaking with slight troughs in the transition region. It is seen that the axial flux peak falls to the random level much more rapidly than in the [0001]-$\{11\bar{2}0\}$ scan, where the peak exhibits distinct wings, although the widths of the two peaks at half-maximum are almost identical. The magnitude of the axial flux peak in both scans is less than for the scan in Fig. 3(a) due to radiation damage, all three scans being performed on the same beam spot.

In the $\langle 11\bar{2}0\rangle$-(0001) scan the behavior of the ^{18}O yield is completely unlike that in the [0001]-$\{10\bar{1}0\}$ scan. Here the planar flux peaking is higher than

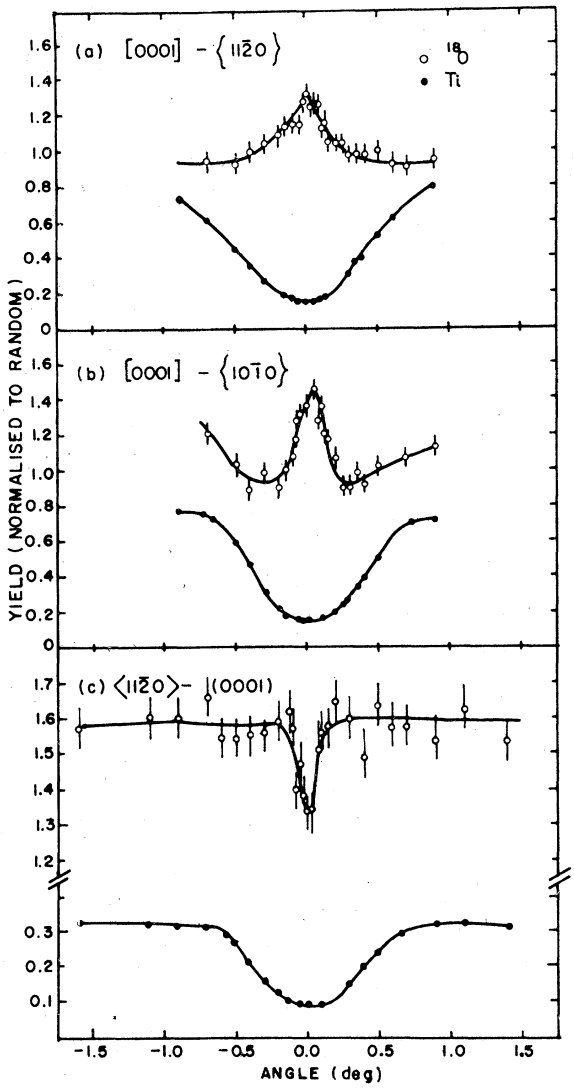

FIG. 6. Angular scans across (a) the [0001] axis in a $\{11\bar{2}0\}$ plane, (b) the [0001] axis in a $\{10\bar{1}0\}$ plane, and (c) a $\langle 11\bar{2}0\rangle$ axis in the (0001) plane, with the same conditions as for Fig. 3.

the axial, as noted previously, with the yield showing an extremely narrow dip (width 0.13°) at the axis. A similar effect was observed by Della Mea *et al.*[5] for deuteron channeling in $TiO_{0.11}$, but in this case the O concentration is sufficiently high to perturb the axial flux peaking significantly. To our knowledge, such an effect has not been observed previously at low impurity concentrations.

In order to investigate the origin of this effect, theoretical calculations of the flux peaking for 730-keV protons in a $\langle 110\rangle$-$\{111\}$ angular scan in Cu were performed. The channeling critical angles for the $\langle 110\rangle$ channels in Cu and the $\langle 11\bar{2}0\rangle$ channels in Ti differ by ~20%, and as can be seen from Figs. 2 and 7, the shapes of the channels are almost iden-

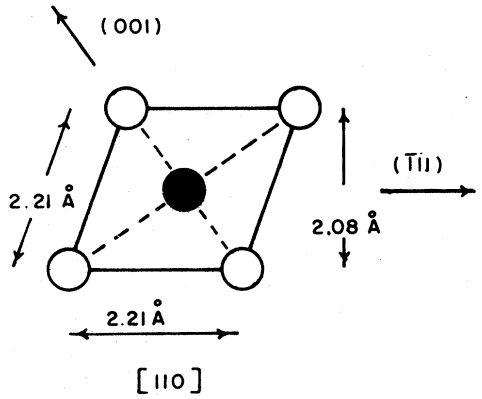

FIG. 7. Cross section of a [110] axial channel in Cu, for which computer simulations of flux peaking were performed. Open circles represent rows of Cu atoms, and the filled circle denotes the projection of the octahedral interstitial site on a plane normal to the channel.

tical. There is a slight asymmetry in the Ti $\langle 11\bar{2}0\rangle$ channels about the channel diagonals, but the deviation of ~2% from perfect symmetry should have a negligible influence on the flux peaking. The (0001) plane in Ti corresponds to the $\{111\}$ planes in Cu, the octahedral site lying at the channel center in both cases.

The calculations were of two types: (a) analytical calculations based on a multirow continuum model, and (b) Monte Carlo computer simulations based on a binary-collision model. The analytical model is the same as that described in Refs. 25 and 26. Statistical equilibrium is assumed and no allowance is made for depth effects associated with nuclear and electronic multiple scattering. However, the implanted O is close to the surface, and the flux peaking is averaged over a depth of ~1000 Å experimentally due to the limited depth resolution. Details of the Monte Carlo computer program, which includes multiple scattering, are given elsewhere.[8,25] Values of the program parameters were chosen to correspond to those for the experimental measurements in Ti; the flux for 625 incident particles was averaged over a depth of 1000 Å from the crystal surface. For the analytical calculations the standard Lindhard row and plane potentials were used, while the computer simulations employed the Molière interatomic potential. In both sets of computations, the flux was averaged over the area of a square of side ±0.09 Å(cf. $x_{rms} = 0.078$ Å in Cu at 20 °C) centered on the octahedral site.

In the analytical calculations, the flux-peak magnitudes for the $\langle 110\rangle$ axis and $\{111\}$ plane were found to be 2.59 and 1.57, respectively. As a specific tilting plane cannot be chosen in the model used, it was not possible to follow the transition from the axis to the plane. However, the calculated planar flux peak is lower than the axial, in contrast to the experimental results for the $\langle 11\bar{2}0\rangle$-(0001) transition in Ti.

A similar result was obtained in the computer simulations, as shown in Fig. 8. For comparison,

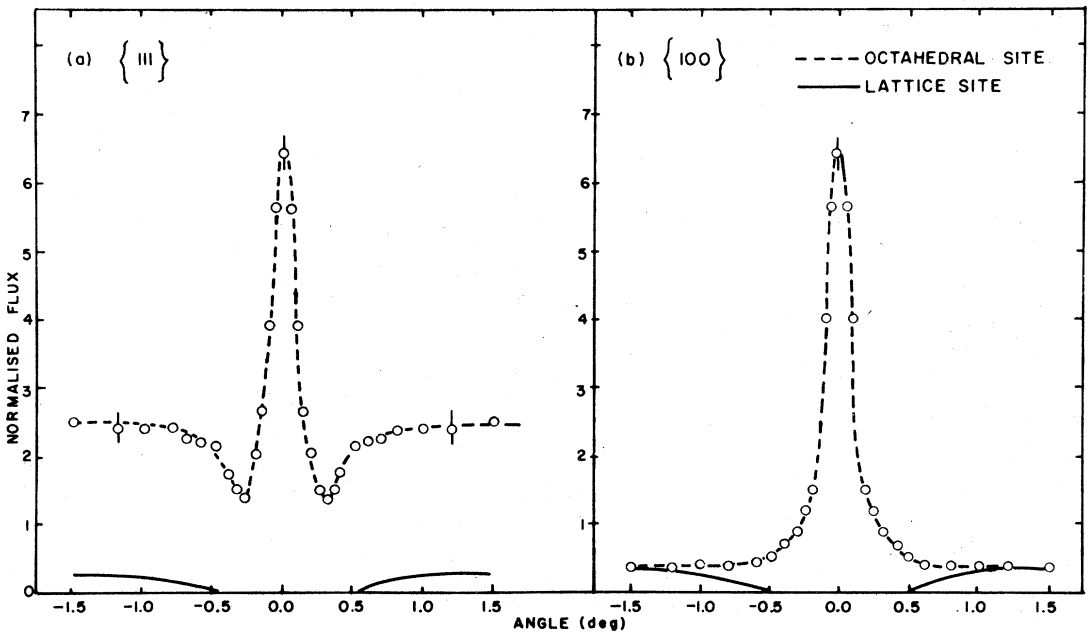

FIG. 8. Computer simulations of the ion flux at the octahedral interstitial site and at a lattice site in Cu, for scans across a $\langle 110\rangle$ axis in (a) a $\{111\}$ plane and (b) a $\{100\}$ plane. The flux is calculated for 730-keV protons in Cu at 20 °C, and is averaged over 1000 Å starting from the crystal surface.

a simulated scan was carried out across the ⟨110⟩ axis in a {100} plane, along which the octahedral sites are shadowed. The results of this scan are qualitatively similar to those of the experimental [0001]-{11$\bar{2}$0} scan in Ti [Fig. 6(a)], where the octahedral sites are also shadowed along the planes. The simulated ⟨110⟩-{111} scan is qualitatively similar to the Ti [0001]-{10$\bar{1}$0} scan, though the calculated flux peaking remains above the random level in the transition region. It should be noted that no allowance is made in the calculations for dechanneling associated with radiation damage. A point of interest is that the widths of the peaks in the two scans in Fig. 8 are approximately the same.

Although the magnitudes of the axial and planar flux peaking in the computer simulations are greater than in the analytical calculations, the difference probably arises from the assumption of statistical equilibrium in the analytical model. Computer calculations for a depth of 500 Å gave axial and planar flux peaks which were slightly smaller, but of the same relative magnitude. This indicates that the depth dependence of the flux peaking is similar for the axis and the plane.

There are several possible explanations for the discrepancy between the experimental and calculated Ti ⟨11$\bar{2}$0⟩-(0001) flux-peaking behavior. In the work of Della Mea *et al.*[5,6] on Ti-O alloys, it was shown that axial flux peaking decreases significantly with increasing interstitial O concentration, while planar flux peaking is only weakly affected. Extrapolation of their results suggests that the flux peak for an axis could become less than that for a plane intersecting the axis at an O concentration $\gtrsim$4 at. %. In our work the implanted ^{18}O concentration was only ~0.14 at. % (Sec. IIA), consistent with the measured α-particle yields. It is possible, however, that the crystals contained a relatively large dissolved ^{16}O component. Even for an ^{16}O concentration of 4 at. %, the corresponding ^{18}O concentration would be only 0.01 at. %, comparable to that in the surface oxide layer. The near-surface ^{16}O content of the crystals could in principle be determined by ^{16}O$(d,p)^{17}$O measurements, but the limited depth resolution would make it impossible to distinguish the yield contribution from the surface oxide. Such an explanation of the observed flux-peaking effect seems unlikely, as a similar effect is not seen in the [0001]-{10$\bar{1}$0} scan. Nevertheless, a high O concentration in the ⟨11$\bar{2}$0⟩ crystal alone is possible.

Another possibility is that the thermal vibrational amplitude of O atoms in octahedral sites is larger in a direction parallel to the (0001) plane than it is perpendicular to the plane. This would have the effect of reducing the axial flux peaking but not the planar[23] (cf. Fig. 2). However, the computer simulation results (for Cu) indicate that even if the difference in vibrational amplitudes were a factor of 2, the axial flux peak would still be higher than the planar.

It seems likely that the explanation lies in the potentials used in the calculations. It is well recognized that potentials such as the average Lindhard and Molière potentials may not be good approximations at large distances from lattice atoms, especially near the center of a channel where flux peaking occurs. If the ⟨11$\bar{2}$0⟩ transverse potential were slightly flatter at the channel center than either of these two potentials, the calculated flux peak for the axis could be less than that for the intersecting (0001) plane. A similar effect might not occur for the [0001] axis, where the potential has a different shape about the channel center.

IV. CONCLUSIONS

The major results of this study are as follows: (i) As expected, the magnitude of a flux peak is extremely sensitive to any factors which increase the transverse energy of the best-channeled ions. The factors investigated here are the Coulomb explosion of incident molecular ions, and multiple scattering due to radiation damage. Small levels of damage reduce the flux peaking significantly. (ii) The width of a flux peak is relatively insensitive to multiple scattering, as predicted by theoretical models. (iii) The shape of an axial flux peak near the random-yield level varies with the tilting plane, only in so far as the axial flux-peaking site is interstitial or shadowed with respect to the plane. (iv) For 730-keV protons in Ti, the magnitude of the flux peak for the (0001) plane is greater than that for the ⟨11$\bar{2}$0⟩ axis intersected by the plane. This behavior is opposite to that predicted by both analytical calculations and computer simulations for the geometrically similar Cu {111} plane and ⟨110⟩ axis. Of various possible explanations for the discrepancy, the inadequacy of the potentials used in the calculations seems the most likely.

In conclusion, the results should emphasize the difficulties in making accurate quantitative estimates of flux-peaking effects, and the need for improved theoretical models.

ACKNOWLEDGMENTS

We would like to thank W. Temple for performing the implantations, J. Andreassen for his help with construction, and E. Laegsgaard for his valuable experimental advice, We gratefully acknowledge helpful discussions with J. U. Andersen and G. Dearnaley.

*Present address: Dept. of Physics, Wayne State University, Detroit, Michigan 48202.
†Present address: School of Physics, University of Melbourne, Melbourne, Australia.

[1]See, for example, *Channeling*, edited by D. V. Morgan (Wiley, London, 1973); D. S. Gemmell, Rev. Mod. Phys. 46, 129 (1974).
[2]S. T. Picraux, in *New Uses of Ion Accelerators*, edited by J. F. Ziegler (Plenum, New York, 1975), p. 229.
[3]W. M. Gibson, Ann. Rev. Nucl. Sci. 25, 465 (1975).
[4]F. H. Eisen and E. Uggerhøj, Radiat. Eff. 12, 233 (1972).
[5]G. Della Mea, A. V. Drigo, S. Lo Russo, P. Mazzoldi, S. Yamaguchi, G. G. Bentini, A. Desalvo, and R. Rosa, in *Atomic Collisions in Solids*, edited by S. Datz, B. R. Appleton, and C. D. Moak (Plenum, New York, 1975), Vol. 2, p. 791.
[6]G. Della Mea, A. V. Drigo, S. Lo Russo, P. Mazzoldi, S. Yamaguchi, G. G. Bentini, A. Desalvo, and R. Rosa, Phys. Rev. B 10, 1836 (1974).
[7]B. Holmberg, Acta Chem. Scand. 16, 1245 (1962).
[8]R. B. Alexander and J. M. Poate, Radiat. Eff. 12, 211 (1972).
[9]D. Van Vliet, Radiat. Eff. 10, 137 (1971).
[10]C. Erginsoy, Phys. Rev. Lett. 15, 360 (1965).
[11]H. E. Schiøtt, Radiat. Eff. 6, 107 (1970).
[12]S. S. Mozhaev and L. F. Sokiryanskii, in *Titanium and its Alloys*, edited by I. I. Kornilov (Israel Programme for Scientific Translations, Jerusalem, 1963), p. 137.
[13]G. Amsel and D. Samuel, Anal. Chem. 39, 1689 (1967).
[14]G. Amsel, J. P. Nadai, E. d'Artemare, D. David, E. Girard, and J. Moulin, Nucl. Instrum. Methods 92, 481 (1971).
[15]J. H. Barrett, Phys. Rev. B 3, 1527 (1971).
[16]M. A. Kumakhov, Dokl. Akad. Nauk SSSR 203, 794 (1972) [Sov. Phys. Dokl. 17, 348 (1972)].
[17]M. A. Kumakhov, Radiat. Eff. 15, 85 (1972).
[18]J. M. Caywood, T. A. Tombrello, and T. A. Weaver, Phys. Lett. A 37, 350 (1971).
[19]T. A. Tombrello and J. M. Caywood, Phys. Rev. B 8, 3065 (1973).
[20]M. J. Gaillard, J.-C. Poizat, A. Ratkowski, and J. Remillieux, Nucl. Instrum. Methods 132, 69 (1976).
[21]See, for example, D. S. Gemmell, J. Remillieux, J.-C. Poizat, M. J. Gaillard, R. E. Holland, and Z. Vager, Nucl. Instrum. Methods 132, 61 (1976); W. Brandt and R. H. Ritchie, Nucl. Instrum. Methods 132, 43 (1976).
[22]J. U. Andersen, O. Andreasen, J. A. Davies, and E. Uggerhøj, Radiat. Eff. 7, 25 (1971).
[23]S. T. Picraux, in *Ion Beam Surface Layer Analysis*, edited by O. Meyer, G. Linker, and F. Kappeler (Plenum, New York, 1976), p. 527.
[24]D. V. Morgan and D. Van Vliet, Radiat. Eff. 5, 157 (1970).
[25]R. B. Alexander, P. T. Callaghan, and J. M. Poate, Phys. Rev. B 9, 3022 (1974).
[26]P. T. Callaghan, P. K. James, and N. J. Stone, Phys. Rev. B 12, 3553 (1975).